Liquefaction assessment of gravelly soils: the role of in situ and laboratory geotechnical tests through the case study of the Sulmona basin (Central Italy)

NADIA SALVATORE, ALBERTO PIZZI, KYLE M. ROLLINS, ALESSANDRO PAGLIAROLI, SARA AMOROSO

Nadia Salvatore - Department of Engineering and Geology, University. "G. d'Annunzio" of Chieti-Pescara, via dei Vestini, 31, 66100 Chieti, Italy. ORCID: 0000-0002-9240-9270. Corresponding author, e-mail: nadia.salvatore@unich.it

Alberto Pizzi – Associate Professor, Department of Engineering and Geology, University. "G. d'Annunzio" of Chieti-Pescara, via dei Vestini, 31, 66100 Chieti, Italy. ORCID: 0000-0002-5196-4956. e-mail: alberto.pizzi@unich.it

Kyle M. Rollins – Full Professor, Department of Civil and Environmental Engineering, Brigham Young University, 368 CB, Provo, UT 84602. ORCID: 0000-0002-8977-6619. e-mail: rollinsk@byu.edu

Alessandro Pagliaroli – Associate Professor, Department of Engineering and Geology, University. "G. d'Annunzio" of Chieti-Pescara, viale Pindaro, 42, 65129 Pescara, Italy ORCID: 0000-0002-7431-5094. e-mail: alessandro.pagliaroli@unich.it

Sara Amoroso – Assistant Professor, Department of Engineering and Geology, University. "G. d'Annunzio" of Chieti-Pescara, viale Pindaro, 42, 65129 Pescara, Italy; Research Associate, Istituto Nazionale di Geofisica e Vulcanologia, Italy ORCID: 0000-0001-5835-079X. e-mail: sara.amoroso@unich.it

ABSTRACT

Even though liquefaction in gravelly soil is well documented in many earthquakes since 1891, most of the "simplified procedures" and national buildings codes still consider only sandy soil liquefaction in seismic hazard assessment. In this study, 109 sites of gravel liquefaction related to 27 historical earthquakes from 1891 to 2020 are reported, with a wide range of moment magnitudes, M_W, (5.3 to 9.2) and focal depths (5.4 to 33 km), highlighting the potential for liquefaction of gravelly soils even

during moderate earthquakes. Although gravels are often thought to have hydraulic conductivities high enough to preclude liquefaction, gravels that have liquefied are generally well-graded sandy gravels. The sand content is typically 30% or more so that the hydraulic conductivity is governed by the sand size making them clearly liquefiable. Even for gravels with lower sand contents, a low permeability surface layer has often been observed that could restrict drainage and produce excess pore pressure during strong shaking.

The epicentral distance calculated for every gravel liquefaction site plotted vs the magnitude of the earthquake event shows a pattern which closely follows similar curves provided in the literature for sandy soils. However, field observations of liquefaction in gravelly soils are less frequent in the historical record.

In addition to examining gravel liquefaction sites in general, this paper provides a case history illustrating the difficulties of liquefaction assessment in gravels at a site in Santa Rufina (Sulmona basin, Central Italy). This site, characterised by high vertical and lateral stratigraphic variability, was selected for gravel liquefaction assessment using a combination of *in-situ* tests, laboratory geotechnical analysis, and geological studies. We found that, even if SPT- and DPT- based *in-situ* methods provide conflicting results, the availability of a borehole log, along with standard laboratory test results, proved to be fundamental to achieving a reliable assessment of the liquefaction hazard.

KEY WORDS: *Gravel liquefaction, dynamic cone penetration test, geotechnical laboratory tests, Sulmona basin, Holocene alluvial deposits.*

INTRODUCTION

During major earthquakes, the impact of soil liquefaction on social and economic losses is well documented in historical records (e.g., Baratta, 1910). The reduction of stiffness and shear strength following liquefaction of loose water-saturated cohesionless soils during earthquake shaking may induce damage to buildings, infrastructure, or pipelines, and ignite fires due to gas line breaks.

Obermeier (1996) underlined the importance of combining geological and geotechnical approaches to properly interpret liquefaction processes. This is still a key requirement for geologists and engineers who try to develop effective techniques to predict the susceptibility of soils to this phenomenon, even when focusing their attention mostly on sandy soils, e.g., Idriss & Boulanger (2008), Boulanger & Idriss (2014).

Tsuchida & Hayashi (1971) first proposed a relationship between grain size and susceptibility to liquefaction, plotting the grain-size distribution soils at Japanese liquefaction sites and tracing the grain-size boundaries of the most liquefiable and potentially liquefiable soils, in combination with the uniformity coefficient, C_U. These grain-size boundaries for liquefiable soil are still widely used and are included in national building codes, such as those for Italy (NTC, 2018). However, these liquefaction susceptibility boundaries do not include gravelly soils that have been observed to liquefy in well document cases all over the world, especially over the past 10 years (Salocchi *et* alii, 2020; Rollins *et alii,* 2021).

This paper summarises knowledge gained from studies of gravel liquefaction case histories throughout the world in a concise state-of-the-art section. It then highlights the importance of liquefaction assessment in gravelly soils using a multidisciplinary approach that integrates geological and geotechnical information. Emphasis is given to laboratory and in situ geotechnical tests that may improve fundamental understanding of the liquefaction susceptibility of gravels, as illustrated by the case study at Santa Rufina (Sulmona basin, Central Italy).

LIQUEFACTION OF GRAVELLY SOILS: THE STATE-OF-ART

While techniques for liquefaction assessment in sandy soils were developed in the second half of the 20th century (e.g., Seed & Idriss, 1971; Tsuchida & Hayashi, 1971; Amoroso *et alii*, 2017, 2020), the liquefaction phenomena in gravelly soils were not evaluated with a probabilistic analysis until the 2008 Wenchuan (China) earthquake (Cao *et alii,* 2011).

Nevertheless, gravel liquefaction during earthquakes has been observed all over the world, as illustrated in Fig. 1, since the 1891 Mino-Owari (Japan) earthquake (Tokimatsu & Yoshimi, 1983). Therefore, the evidence for gravel liquefaction is not so uncommon and is not only associated with strong events.

Table S1 reports the gravel liquefaction dataset with the location of 109 sites where researchers have identified gravel liquefaction phenomena related to 27 historical earthquakes from 1891 to 2020. These liquefaction case histories sites are located at epicentral distances ranging from ~1.5 to ~215 km, and involve earthquakes with a wide range of moment magnitudes (M_W) (from 5.3 to 9.2), and focal depths (from 5.4 to 33 km). Compared to Rollins *et alii*, 2021, the earthquake case history list has been expanded with two more events (the M_W 6.3, 2020 Petrinja (Croatia – Amoroso *et alii*, 2021; Baize *et alii*, 2022) and the M_W 5.5, 2017 Pohang (South Korea – Naik *et alii*, 2019) earthquakes) and the liquefaction site database has been expanded with 29 more sites. In addition, accurate geographical coordinates have been added for each site by bibliographic research. Furthermore, magnitude values were standardized to M_W using databases from the United States Geological Survey (USGS), the Istituto Nazionale di Geofisica e Vulcanologia (INGV), the Parametric Catalogue of Italian Earthquakes (Rovida *et alii*, 2022), and the Geological hazard information for New Zealand (GeoNet). The epicenters were identified by their coordinates, as reported by the abovementioned databases. Where possible, we also characterised the seismic source by the fault plane solution (Fig. 1), as reported by USGS, INGV, and GeoNet, or by bibliographic research (Table S1).

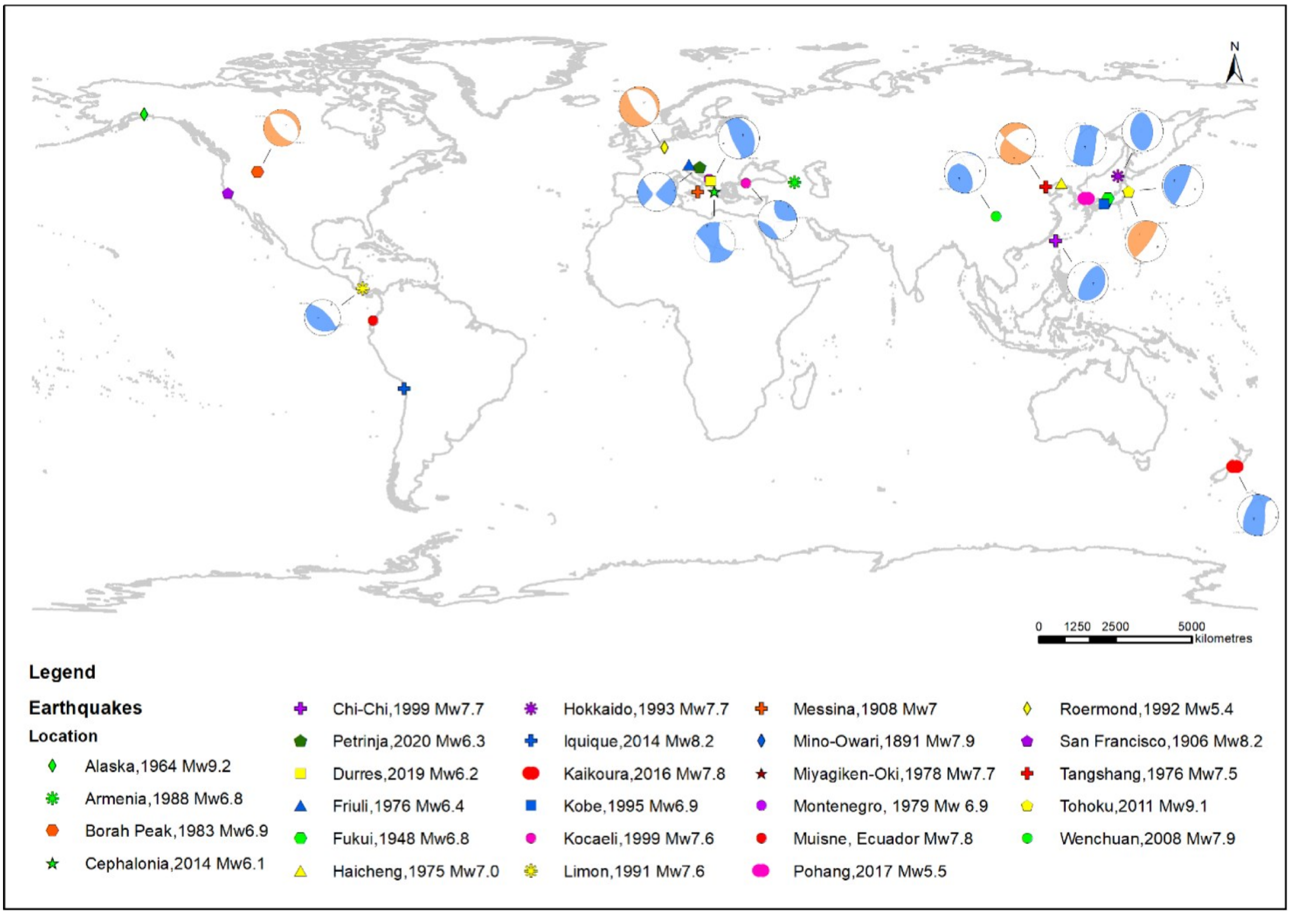

Fig. 1 – World map of gravel liquefaction case histories. The beach balls represent the fault plane solution as moment tensor (blue), or focal mechanism (orange) as reported by the USGS. The magnitude values indicated are from USGS, INGV and GeoNet databases.

To compare the liquefaction susceptibility of sands and gravels, we have used the gravel case history database to develop magnitude vs. epicentral distance to liquefaction sites for gravels for a range of magnitudes around the world. We have then compared the resulting pattern with the magnitude vs epicentral distance to liquefaction curves proposed for sand by various authors. These gravel liquefaction data points have been plotted as black circles in the magnitude vs. epicentral distance plot in Fig. 2 along with curves showing the boundary curves for sand proposed by various researchers. A comparison of gravel data points and the boundary curves for sand, shows that: (a) gravel liquefaction is not only associated with strong events, and (b) that the boundary for the gravel liquefaction data is quite similar to the boundary curves for sand provided in the literature from four researchers.

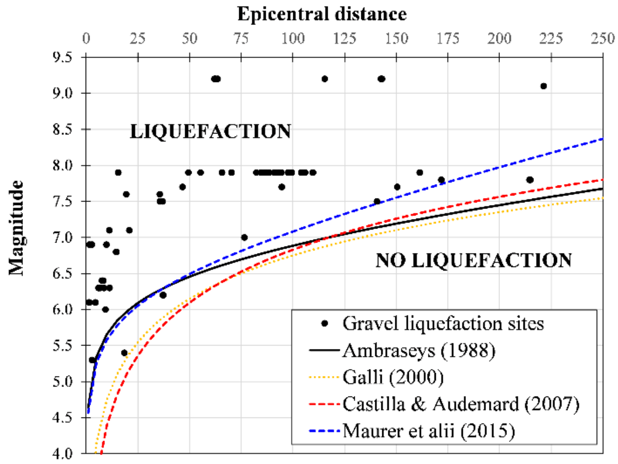

Fig. 2 – Chart of magnitude vs. epicentral distance to gravel liquefaction sites and available reference correlations (Ambraseys, 1988; Galli, 2000, Castilla & Audemard, 2007, Maurer *et alii*, 2015) based on sand liquefaction sites.

Regarding the first point, liquefaction in gravelly soils can be induced by moderate events, as illustrated by a M_W 5.3 aftershock of the 1976-1977 Friuli (Italy) seismic sequence (Sirovich, 1996; Rollins *et alii*, 2020) or by the M_W 5.5, 2017 Pohang earthquake (Naik *et alii*, 2019), although this contradicts with several previous studies (e.g., Obermeier, 1996; Rodriguez-Pascua *et alii,* 2000) which suggested that gravel liquefaction can only be triggered by strong seismic events (magnitude $M > 7$).

Regarding the second point, we observe that the magnitude/epicentral distance pattern for our gravelly soils dataset approximately follows the boundary curve proposed by Maurer *et alii* (2015). This suggests the possibility of liquefaction, at a given epicentral distance and for a given magnitude, is almost the same for both sandy and gravelly soils.

Grain-size distribution curves of liquefied gravels are available for some of the case histories reported in Table S1. A comparison between the grain-size boundaries defined by gravel liquefaction data (yellow bold lines in Fig. 3a) and for sand liquefaction by Tsuchida & Hayashi (1971) shows that there is a limited overlap for the liquefaction susceptibility ranges. Liquefied soils are classified mainly as well-graded gravel (GW) with a gravel content (> 4.75 mm) between 14 and 82% and fines content (FC) ≤ 22%, as reported in Table 1. It is important to note that the liquefied gravels are typically well-graded sandy gravels with $C_U > 3.5$ in all the analysed case histories. In addition, they typically contain more than 30% sand. Gravels are often thought to have hydraulic conductivities high enough (>0.004 m/s) that excess pore pressures would dissipate as fast as they generate in an earthquake (Seed *et alii*, 1976). However, for gravels containing more than 30% sand size particles, the hydraulic conductivity would likely be controlled by the D_{10} (diameter in the grain size distribution corresponding to 10% finer) size of the sand, making the sandy gravel susceptible to liquefaction. Even for gravel sites with higher hydraulic conductivities, the presence of a low-permeability surface layer could impede drainage and make the gravel susceptible to liquefaction (Cao *et alii*, 2013).

Table 1 – Grain size information of liquefied gravels at the available world case histories.

Earthquake	***Sample***	***> 4.75 mm (%)***	***FC (%)***	***D_{60} (mm)***	***D_{30} (mm)***	***D_{10} (mm)***	***C_U (-)***	***C_C (-)***	***USCS classific.***
1964 Alaska (USA)	Old Valdez	14	12.0	1.213	0.255	< 0.075	> 3.5	-	SW-SM
	Old Valdez	58	5.6	11.529	2.690	0.316	36.5	2.0	GW-GM
	Valdez	46	6.8	7.133	2.152	0.228	31.2	2.8	SW-SM
	Seward	74	1.7	20.221	3.149	0.427	47.4	1.1	GW
1976 Friuli (Italy)	Avasinis	21	13.0	1.949	0.466	< 0.075	> 3.5	-	SM-SC
	Avasinis	42	10.0	5.320	1.181	0.075	70.9	3.5	SW-SM
1985 Borah Peak, Idaho (USA)	Pence Ranch	51	4.0	8.033	1.791	0.293	27.3	1.4	GW
	Larter Ranch	66	4.0	16.184	3.570	0.478	33.8	1.6	GW
	Whiskey Springs	52	20.0	8.330	0.708	< 0.075	> 3.5	-	GM-GC
2008 Wenchuan (China)	China	23	12.0	1.182	0.221	< 0.075	> 3.5	-	SW-SM
	China	69	10.0	42.943	4.509	0.075	572.6	6.3	GW-GM
2016 Muisne (Ecuador)	Manta	82	5.7	15.600	5.303	0.226	68.9	8.0	GW-GM
	Manta	35	21.7	3.364	0.191	< 0.075	> 3.5	-	SM-SC
2016 Wellington (New Zealand)	Wellington	77	0.8	17.514	7.350	1.738	10.1	1.8	GW
	Wellington	34	22.0	3.414	0.154	< 0.075	> 3.5	-	SM-SC

Notes: FC is the fines content; D_{60}, D_{30}, and D_{10} are the 60th, 30th, and 10th percentiles of the grain size curve; C_U is the coefficient of uniformity; C_C is the coefficient of curvature; USCS is the Unified Soil Classification System according to ASTM D2487-11 (2011) (SW is clean well-graded sand; SM is silty sand; SC is clayey sand; GW is well-graded gravel; GM is silty gravel; GC is clayey gravel)

The geotechnical laboratory characterisation of gravelly soils has always been a challenge because of the difficulties in taking undisturbed or partly disturbed samples with a large enough diameter to provide a representative sample. In this respect the first attempts in liquefaction assessment of gravelly soils were made by performing the classical *in-situ* tests, such as the Standard Penetration Test (SPT).

Seed & Idriss (1971) defined the cyclic resistance ratio, ($CRR_{7.5}$), as the capacity of the soil to resist liquefaction for a magnitude 7.5 earthquake and developed corelations to define $CRR_{7.5}$ using *in-situ* tests. They also defined the cyclic stress ratio (CSR), meaning the seismic demand on a soil layer by an earthquake that can be normalised to a magnitude of 7.5, namely $CSR_{7.5}$, through the magnitude scaling factor (MSF), used as a "proxy" for duration effects on triggering liquefaction. To consider also high effective overburden stress, Youd *et alii* (2001) proposed the overburden correction factor (K_{σ}), to further correct the cyclic stress ratio to $CSR_{7.5,1\ atm}$ at one atmosphere. This led to the definition of the threshold value for liquefaction, namely the safety factor against liquefaction (FS_{liq}) as the ratio between $CRR_{7.5}$ and $CSR_{7.5,1\ atm}$.

Youd *et alii* (2001) proposed an SPT procedure for liquefaction assessment in sandy soils, using the corrected SPT blow count, $(N_1)_{60}$, that is a normalized value of the SPT blow count (N_{SPT}). This procedure was updated by Idriss & Boulanger (2008), and more recently by Boulanger & Idriss (2014).

Although the use of the SPT-based approach correctly estimates the liquefaction potential in loose gravel with low penetration resistance, after the application of a correction factor (e.g., Kokusho & Yoshida, 1997), the results may be inaccurate when the penetration resistance increases. In this case it is not always possible to discriminate if the increased blow count is due to the presence of large coarse particles or to the increase in soil density (Daniel *et alii*, 2003; Cubrinovsky *et alii*, 2018; Rollins *et alii*, 2021). This problem could be bypassed by correlating liquefaction resistance with the shear wave velocity (V_S) as proposed by Andrus & Stokoe (2000) and Kayen *et alii* (2013) for sandy soils. However, several studies have shown that (1) the $V_S$boundaries for liquefaction triggering may be higher for gravels with respect to sands (e.g., Cao *et alii*, 2013), and that (2) the V_S measurements are related to small strains while liquefaction occurs at medium-high strains that are better represented by penetration tests (e.g., Mayne *et alii,* 2009). Nevertheless, Cao *et alii* (2011) and more recently Rollins *et alii* (2022) have developed probabilistic liquefaction triggering curves based on V_S data from the gravel liquefaction case history database.

New penetrometers with larger diameters are required to overcome problems associated with SPT tests in the presence of large particles and to evaluate the *in-situ* liquefaction resistance of gravelly soils. The Becker penetration test (BPT), developed in Canada in the 1950s, is the first and most widely used equipment in the North America (Youd *et alii*, 2001) for liquefaction assessment of gravelly soil. However, the test is expensive and not easily available, and the BPT results need to be converted to an "equivalent" SPT blow count to assess liquefaction (e.g., Rollins *et alii,* 2021).

At the same time, Chinese engineers developed the dynamic cone penetration test (DPT), that consists of a 74 mm cone driven continuously by a 120 kg hammer dropped from one metre, using a drilling rig or a simple SPT tripod system (Chinese Design Code, 2001). As with the SPT, the DPT requires the measurement of the hammer efficiency by determining the energy transfer ratio (ER), defined as the ratio of the energy transferred from the hammer to the rods relative to the theoretical free-fall energy, in order to correct the raw DPT blow counts. Moreover, DPT blow counts are normalised to include a correction for the overburden stress using the equation:

$$N'_{120} = N_{120}(100/\sigma'_v)^{0.5} \tag{1}$$

where N'_{120} is the corrected DPT resistance in blows per 30 cm, N_{120} is the measured DPT resistance in blows per 30 cm multiplied by ER, 100 is the atmospheric pressure in kPa and σ'_v is the effective overburden stress in kPa.

DPT tests have been carried out at gravel liquefaction sites related to the M_W 7.9 Wenchuan earthquake to develop a probabilistic DPT-based procedure to assess liquefaction (Cao *et alii,* 2013). The authors use the same $CSR_{7.5}$ definition proposed by Youd *et alii* (2001), although it is not established if the MSF correction is appropriate also for gravelly soils (Rollins *et alii*, 2021). To define the $CRR_{7.5}$, DPT blow count data were analysed using the logistic regression procedure by Liao *et al* (1988), and obtained the probability function for liquefaction (P_L):

$$\ln[P_L/(1 - P_L)] = -8.40 + 0.35N'_{120} - 2.12\ln(CRR_{7.5}) \tag{2}$$

Substituting the P_L value (85%, 70%, 50%, 30%, 15%) in equation (2) makes it possible to evaluate the capacity of the soil to resist liquefaction through the $CRR_{7.5}$.

Rollins *et alii* (2021) expanded the DPT database considering 137 sites (80 liquefaction site and 57 no-liquefaction sites) referred to 10 seismic events with a magnitude range from 5.8 to 9.2 from seven countries, including those from Cao *et alii* (2013), and recalculated the triggering curves of the liquefaction probability function.

As in Cao *et alii* (2013), the N_{120} is defined as the measured DPT resistance in blows every 0.3 m multiplied by ER, while the N'_{120} was calculated by adding a threshold value of 1.7 to make the equation proposed by Cao *et alii* (2013) consistent with the C_N value from Youd *et alii* (2001), as follows:

$$N'_{120} = N_{120} C_N \tag{3}$$

where:

$$C_N = (100/\sigma'_{v0})^{0.5} \leq 1.7 \tag{4}$$

where σ'_{v0} is the effective overburden stress in kPa. The CSR was defined according to the formulation proposed by the "simplified procedure" (Seed & Idriss, 1971), including the dependency of the r_d value with magnitude according to the Idriss & Boulanger (2008) formulation. To reduce the various M_W to the standard CSR value of 7.5, $CSR_{7.5}$, Rollins *et alii* (2021) proposed a new MSF correction factor:

$$MSF = 7.258exp(-0.264M_w) \tag{5}$$

For the $CRR_{7.5}$ a logistic regression analysis was performed, to define the probability of liquefaction occurring P_L:

$$P_L = \frac{1}{1 + exp[0.0008N'^{3}_{120} - 1.32M_w - 5.2\ln(CRR_{7.5})]} \tag{6}$$

Fig. 3b provides a comparison of the DPT-based gravel liquefaction triggering curves proposed by Cao *et alii* (2013) and Rollins *et alii* (2021). As may be observed in Fig. 3b, the probabilistic triggering curves from Rollins *et alii* (2021), intercept the $CSR_{7.5}$ axis at values in the range 0.1 - 0.2, providing compatibility with the results obtaining with the SPT; moreover, the use of both additional liquefaction and no-liquefaction data points has reduced the spread between the triggering curves compared to those by Cao *et alii* (2013), thereby decreasing the uncertainty in determination of liquefaction potential of gravelly soils (Rollins *et alii*, 2021).

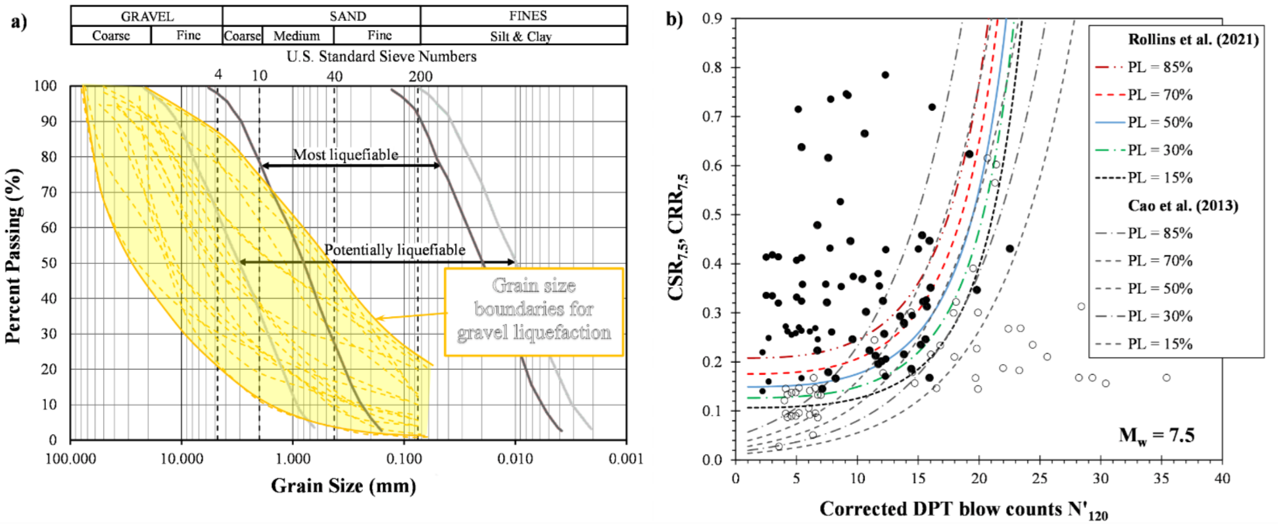

Fig. 3 – a) Gradation curves of liquefied gravelly soils (dashed yellow lines, modified after Rollins *et alii*, 2021). The chart proposes grain size boundaries for gravel liquefaction in comparison with the grain size ranges proposed by Tsuchida & Hayashi (1971) for the most susceptible soils to liquefaction and potentially susceptible soils to liquefaction using a coefficient of uniformity $C_U > 3.5$. b) DPT-based gravel liquefaction chart by Rollins *et alii* (2021) and Cao *et alii* (2013) at different liquefaction probability (P_L).

THE CASE STUDY OF THE SULMONA BASIN

GEOLOGICAL AND SEISMOLOGICAL SETTING

The Sulmona basin (Fig. 4) is an intramountain tectonic depression caused by the Quaternary activity of a normal fault system affecting the western slope of Mt. Morrone (Miccadei *et alii*, 1998; Galli *et alii*, 2015). This system consists of two main sub-parallel faults striking northwest-southeast and dipping to the south-west. The western fault generally marks the boundary between the Meso-Cenozoic carbonate bedrock at its footwall and the Quaternary slope consisting of alluvial and lacustrine deposits on the hanging wall block (Gori *et alii,* 2011; Galli *et alii,* 2015). The occurrence of minor, north-east dipping, antithetic faults is limited only to the northern sector of the basin, which for this reason can essentially be defined as a half-graben.

The historical seismogenic nature of the Mt. Morrone fault system was first suggested by Ceccaroni *et alii* (2009) who, based on archeoseismological studies, hypothesised that it was the probable source of the historical 2nd century A.D strong seismic event. Galli *et alii* (2015) also provided evidence for this contention from a paleoseismological study. Based on an empirical relationship, the seismogenic potential attributed to this source has been estimated to be M_W 6.5-6.7 (Gori *et alii*, 2011; Pizzi *et alii*, 2002; Valentini *et alii,* 2019), with a recurrence time of 2.4 ± 0.2 ka (Galli *et alii*, 2015).

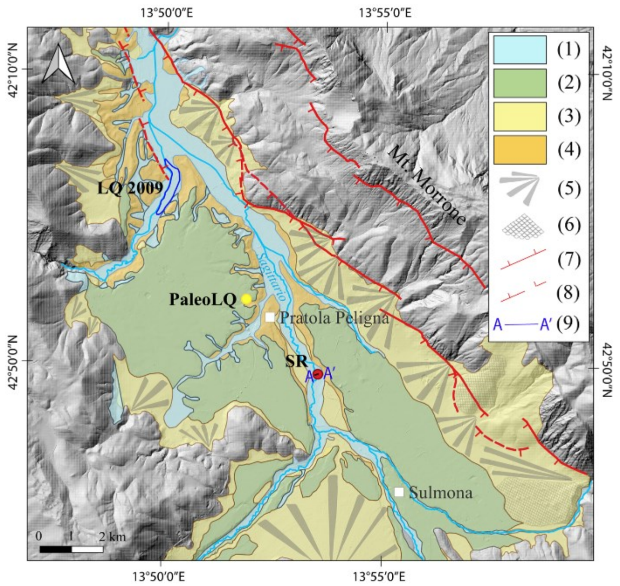

Fig. 4 – Simplified geological map of the Sulmona Quaternary basin, modified from Galli *et alii* (2015), draped on the 10 m resolution DTM by Regione Abruzzo (http://opendata.regione.abruzzo.it/opendata/Modello_digitale_del_terreno_risoluzione_10x10_metri); (1) post-36 ka Upper Pleistocene - Holocene alluvial deposit; (2) ?Middle - Upper Pleistocene (Upper Sulmona Terrace: UST) alluvial and colluvial deposit; (3) Upper Pleistocene (pre-36 ka) fluvial-alluvial, slope fan and landslide deposit; (4) Lower-early Upper Pleistocene lacustrine deposit; (5) alluvial fan; (6) landslide; (7) active normal fault; (8) inferred active normal fault splay; (9) trace of geological cross section; LQ 2009 (blue line) is the area of sand liquefaction near Vittorito village during the M_W 6.1 L'Aquila earthquake (Monaco *et alii*, 2011); PaleoLQ (yellow dot) indicates the site of the presumed gravel paleoliquefaction in Pratola Peligna (AQ); SR (red dot) indicates the DPT test site of Santa Rufina (AQ), grey areas are mainly characterised by outcrops of the pre-Quaternary bedrock.

According to Miccadei *et alii* (1998) the Sulmona basin is mainly filled by lacustrine deposits and subordinately alluvial and slope deposits dating back to the Lower Pleistocene, although the entire sequence of the Quaternary filling has never been observed in either an outcrop or in a borehole to define its thickness.

Recent studies dating the tephra layers within the Sulmona basin infill, based on ${}^{40}Ar/{}^{39}Ar$ methods provided new constraints on the age of the boundary between the top of the fine-grained lacustrine and the bottom of the coarse grained fluvial-alluvial sediments of the Upper Sulmona Terrace (UST) at about 92-100 ka (Giaccio *et alii*, 2013, Galli *et alii*, 2015). The same authors also provided an age of about 36 ka for the top of the UST deposit and the beginning of the intense erosional phase during which the Aterno and Sagittario rivers deeply carved the Upper Sulmona Terrace and deposited the post-36 ka Upper Pleistocene – Holocene alluvial and colluvial deposits in Fig. 4 (e.g., Miccadei *et alii*, 1998).

Borehole data in the Pratola Peligna and Sulmona areas (e.g., seismic microzonation studies, Pizzi *et alii*, 2014), show the first 20 m of the post-36 ka Upper Pleistocene – Holocene alluvial plain consisting of alternating sandy gravel and silt (or sandy silt) layers, sometimes with the presence of soils rich in organic matter. However, there is also significant lateral and vertical variations, as might be expected considering the changes over time in sediment-transport capacity and the path of the riverbed.

LIQUEFACTION SUSCEPTIBILITY BASED ON PRE-EXISTING INFORMATION

During the 6th of April 2009 L'Aquila earthquake (M_W 6.1) the Sulmona basin was affected by liquefaction in an area near the town of Vittorito (LQ2009, Fig. 4), at a distance of about 45 km from the epicenter. In this event, some small sand volcanoes, sand boils and soil cracks with sand ejecta were documented (Monaco *et alii,* 2011). This liquefaction site is near the Aterno riverbed and presents a relatively flat morphology over the Holocene plain deposits. The area was investigated by Monaco *et* alii (2011), who sampled the subsoil by means of two boreholes about 5 m deep and performed three Seismic Dilatometer Tests (SDMT) and one Cone Penetration Test (CPT), to characterise the liquefaction site. The stratigraphic profile consists of a topsoil of about 1 m, followed by a sandy silt layer 2-m thick underlain by a thick sandy layer with some interbedded gravels. The ground water table was detected at about 1.0 m below the ground surface, and the grain-size distribution curves typically plot within the ranges proposed by Tsuchida & Hayashi (1971) for soils most susceptible to liquefaction (Monaco *et* alii, 2011).

At the Pratola Peligna site (Fig. 4) an interesting probable example of gravel paleoliquefaction (Fig. 5) is shown on a recent excavation wall for the construction of an industrial building. The slope face exposes what appears to be a fissure filled by coarse material, that appears to be derived from a gravelly sand layer at its base. The fissure is about 2 m high and 30 cm in width and gravel clasts seem to be distributed along the fracture walls. According to Obermeier (1996), this seems to be comparable with a paleoliquefaction feature related to a seismic event. The origin of the features observable in trenches and outcrops is not easy to determine, as they may originate from various processes, e.g., tectonic fracturing or densification of sediments with the ejection of water and the fluidisation of granular sediments. Further studies are required to exclude syn-depositional processes.

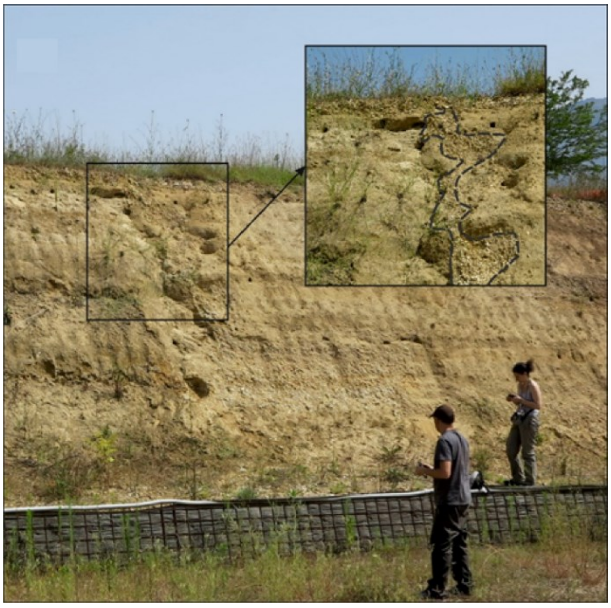

Fig. 5 – Photos from the supposed paleoliquefaction site at Pratola Peligna. The anthropic excavation exposes an alternation of decimetric tabular layers of fluvial – alluvial sands and gravels of the Upper Sulmona Terrace (UST), the black rectangle delimits the part in which a vertical gravelly dike, crossing the entire section, has been recognized. The clasts within the dike are often verticalized and arranged approximately parallel to the dike wall (see the inset). Note that the orientation of the dike surface is at a low angle respect to the excavation wall.

SITE INVESTIGATION AT THE SANTA RUFINA TEST SITE

Considering the liquefaction evidence from the Vittorito and Pratola Peligna sites, the stratigraphic setting of the Pratola Peligna area (Giaccio *et alii*, 2013; Galli *et alii*, 2015), and the possibility of a seismic event of M_W 6.5 in the Sulmona basin (Gori *et alii*, 2011; Pizzi *et alii*, 2002; Valentini *et alii*, 2019), the site in Santa Rufina (SR in Fig. 4) was selected to assess the gravel liquefaction hazard.

This selection was also supported by the availability of a borehole (SB) in the proximity of the study area.

To investigate the potential for gravel liquefaction, a comprehensive geotechnical investigation was performed at the Santa Rufina site, including two DPTs (DPT1, DPT2) and nine SPTs along with a borehole (SR), extending to a depth of 20 m from the ground surface. To better constrain the analysis, 13 disturbed soil samples (CD1 - CD13) were also collected.

Borehole log and laboratory tests

The borehole stratigraphic log (Fig. 6a) confirmed the variability in sediments within the first few meters of the Holocene alluvial plain, showing, under the present topsoil, only a 0.5-m thick layer composed of loose gravel, while the following 3.5 m are mainly composed of silty layers. At 4 m depth, a 1-m thick layer of sandy gravel is encountered, followed by a series of thin layers composed of loose sandy silty fine gravels, sandy clayey silts, and clayey sands down to a depth of 7 m. Then a 2-m thick layer of loose sandy gravel and a 0.6 m layer of fine to coarse loose gravel with sand are detected before reaching a thick layer of grey silt at 9.6 m. Considering the prevalent cohesive nature of the lacustrine sediments below approximately 10 m in depth (Fig. 6a), DPTs and SPTs were limited to the upper 10 m of alluvial sediments. The ground water table (GWT) was intercepted at a depth of 1 m below the ground surface.

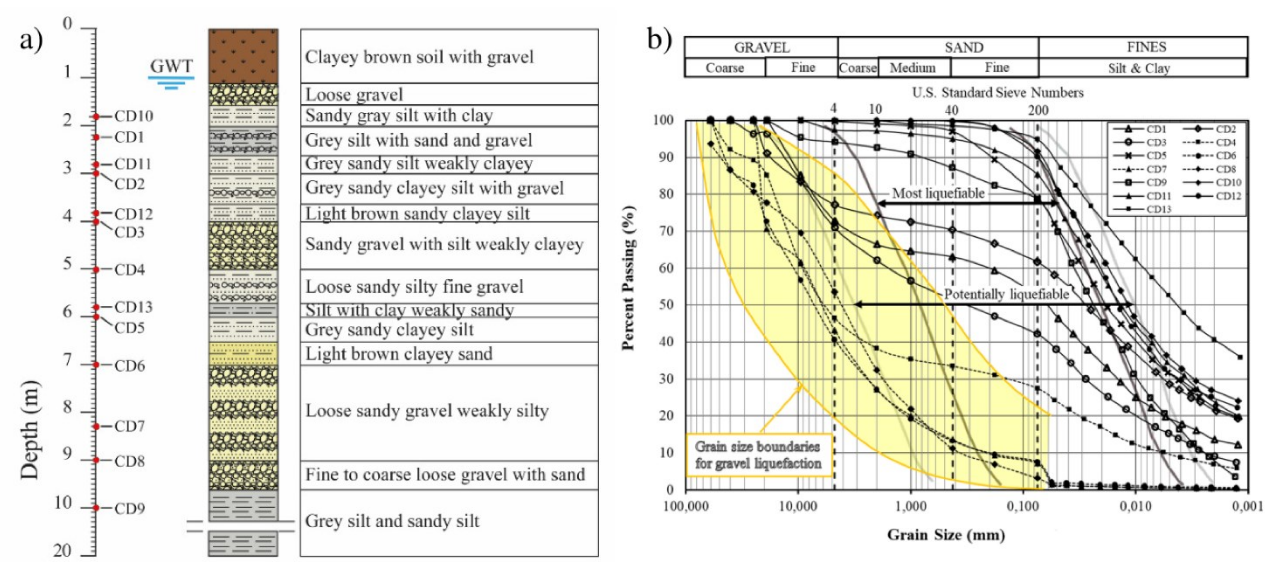

Fig. 6: (a) Stratigraphic log of Santa Rufina (SR) test site: red dots depict samples depth; (b) gradation curves of samples from borehole SR overlaid with the Tsuchida & Hayashi (1971) grain-size charts and with the range of gravel liquefaction susceptibility detected by Rollins *et alii* (2021).

A SW-NE geological section 100 m long and 20 m deep (Fig. 7) was constructed combining subsurface data from boreholes SB and SR with surface geological data from the Geological Map of Italy 1:50.000 (CARG, sheet 369 Sulmona, available on-line at https://www.isprambiente.gov.it/Media/carg/369_SULMONA/Foglio.html) and lithotechnical map available from level 1 Seismic Microzonation studies of Pratola Peligna and Sulmona municipalities (Pizzi *et alii,* 2014). The section at borehole SB shows a surficial 5.5-m thick layer composed of gravelly sand and sandy gravel, followed by 1.5 m of silty sand and then by about 2 m of gravel with clayey sand, 1 m of sand with gravel, 5.5 m of silty clayey sand and 4 m of silty sand and silt.

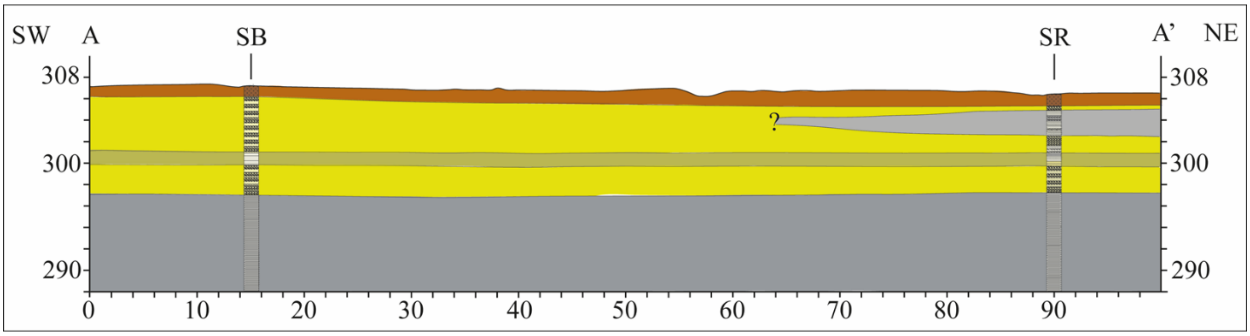

Fig. 7 – Geological section across the Santa Rufina test site; SB is the stratigraphic log of the borehole from pre-existing unpublished studies; SR is the stratigraphic log in Fig. 6a; brown = topsoil; yellow = alluvial deposits composed of sand, gravelly sand, sandy gravel (?Upper Pleistocene - Holocene); dark yellow = alluvial deposits composed of silt and sandy silt (?Upper Pleistocene - Holocene); light grey = alluvial deposits composed of sandy silt sometimes with gravel (?Upper Pleistocene – Holocene) ; grey = lacustrine deposits composed of sandy silt, clayey silt, silt (Middle Pleistocene).

Both SB and SR intercept lacustrine deposits of Middle Pleistocene age at about 10 m, overlaid by ?Upper Pleistocene – Holocene alluvial deposits consisting mostly of sand, sandy gravel, and gravel, with an interbedded thin silty layer. Borehole SR intercepts a 2-m thick layer of sandy silt, not detected in SB, 74 m westward from SR, highlighting the high lateral variability in ?Upper Pleistocene – Holocene alluvial sediments.

The gradation curves resulting from the geotechnical laboratory analyses of 13 samples (Fig. 6b), show a wide variability in grain size; however, all samples are characterised by a $C_U > 3.5$ (Table 2). Gradation curves for the sandy gravel soil samples plot within the range of liquefaction susceptibility identified by Rollins *et alii* (2021) for gravelly soils.

Table 2 – Geotechnical parameters from laboratory tests for Santa Rufina samples.

Sample	***Depth (m)***	***> 4.75 mm (%)***	***FC (%)***	***< 2 µm (%)***	***LL (%)***	***PL (%)***	***PI (%)***	D_{60} ***(mm)***	D_{30} ***(mm)***	D_{10} ***(mm)***	C_U ***(-)***	C_C ***(-)***	***USCS classific.***	***k (m/s)***
CD10	1.90	0.0	91.6	26.7	37	17	20	0.018	-	< 0.0012	> 3.5	-	CL	-
CD1	2.35	27.1	52.5	13.6	30	16	14	0.207	0.014	< 0.0012	> 3.5	-	CL	3.87E-09
CD11	2.90	2.5	85.4	23.8	38	18	20	0.022	0.003	< 0.0012	> 3.5	-	CL	2.40E-10
CD2	3.10	22.8	61.7	21.6	38	18	20	0.063	0.006	< 0.0012	> 3.5	-	CL	-
CD12	3.90	0.0	90.1	24.8	36	17	19	0.021	0.004	< 0.0012	> 3.5	-	CL	-
CD3	4.10	29.0	42.2	9.1	32	17	15	1.519	0.028	0.002	638	0.2	SC	1.88E-09
CD4	5.10	53.5	29.4	7.3	31	18	13	9.044	0.088	0.005	1962	0.2	GC	3.13E-08
CD13	5.90	0.0	94.9	40.7	49	20	29	0.008	-	< 0.0012	> 3.5	-	CL	-
CD5	6.10	0.3	79.0	22.3	37	20	17	0.029	0.004	< 0.0012	> 3.5	-	CL	-
CD6	7.10	59.4	7.2	0.0	-	-	NP	10.99	2.39	0.20	55.7	2.6	GW-GM	-
CD7	8.45	56.8	7.2	0.0	-	-	NP	8.92	2.33	0.20	44.20	3.0	GW-GM	-
CD8	9.15	46.4	3.2	0.0	-	-	NP	6.26	1.71	0.33	19.0	1.4	SW	-
CD9	10.00	5.8	78.8	7.8	50	32	18	0.035	0.010	0.0025	14.3	1.1	MH	3.69E-10

Notes: The sample length is approximately 0.2 m, and the indicated depth represents its average depth. FC is the fines content; LL is the liquid limit, LP is the plastic limit; PI is the plasticity index (NP indicates non-plastic soils); D_{60}, D_{30}, and D_{10} are the 60th, 30th, and 10th percentiles of the grain size curve; C_U is the coefficient of uniformity; C_C is the coefficient of curvature; USCS is the Unified Soil Classification System according to ASTM D2487-11 (2011) (CL is clean clay; MH is elastic silt; SW is clean well-graded sand; SC is clayey sand; GW is well-graded gravel; GM is silty gravel; GC is clayey gravel); k is the coefficient of permeability.

These grain-size distribution curves also highlight the high fines content (FC) of most samples (only the gravelly layers between 7 and 9.6 m in depth are excluded). Furthermore, laboratory analyses show a low permeability value (i.e., $k = 2.40E - 10$) for the layers from 1.6 to 2 m, 2.6 to 4 m, and 5.7 to 6.5 m, which classified as CL according to USCS and which present a plasticity index (PI) between 17 and 29%. In addition, low permeabilities would be expected for the layers from 4 to 5 m and from 5 to 5.7, which classified respectively as SC and GC, with a FC of 42.2 and 29.4% and a PI of 15 and 13%, respectively. It can therefore be assumed that the fines content affects the hydraulic behaviour. The permeability tests in a triaxial cell at constant load were performed on disturbed samples and therefore the k values of Table 2 can be assumed as first order magnitude values. Layers with $FC > 50\%$ were not considered in the liquefaction analyses, except for those "borderline" layers which present FC values near this limit and this will be discussed in the next section.

IN SITU TESTS

To complement the characterisation of the deposits at the Santa Rufina site, the interpreted USCS log is shown in Fig. 8, together with the SPT and DPT blow count profiles in terms of N_{SPT} and N_{120}. The USCS log is derived from laboratory information and visual-manual observations (ASTM D2487-11, 2011; ASTM D2488-09, 2009), while SPTs were performed using a cone tip in the first 9 m, due to the grain size variability from sand to gravel, while a Raymond sampler was used only in the last SPT at 10 m considering the absence of gravels.

The SPT and DPT profiles agree in identifying the presence in the upper 7 m of CL, SC, GC, and GW-GM layers with low resistance to penetration, overlaying a 2 m-thick layer with a higher resistance, corresponding, as can be seen in the USCS log, to the well-graded gravels – silty gravels (GW-GM).

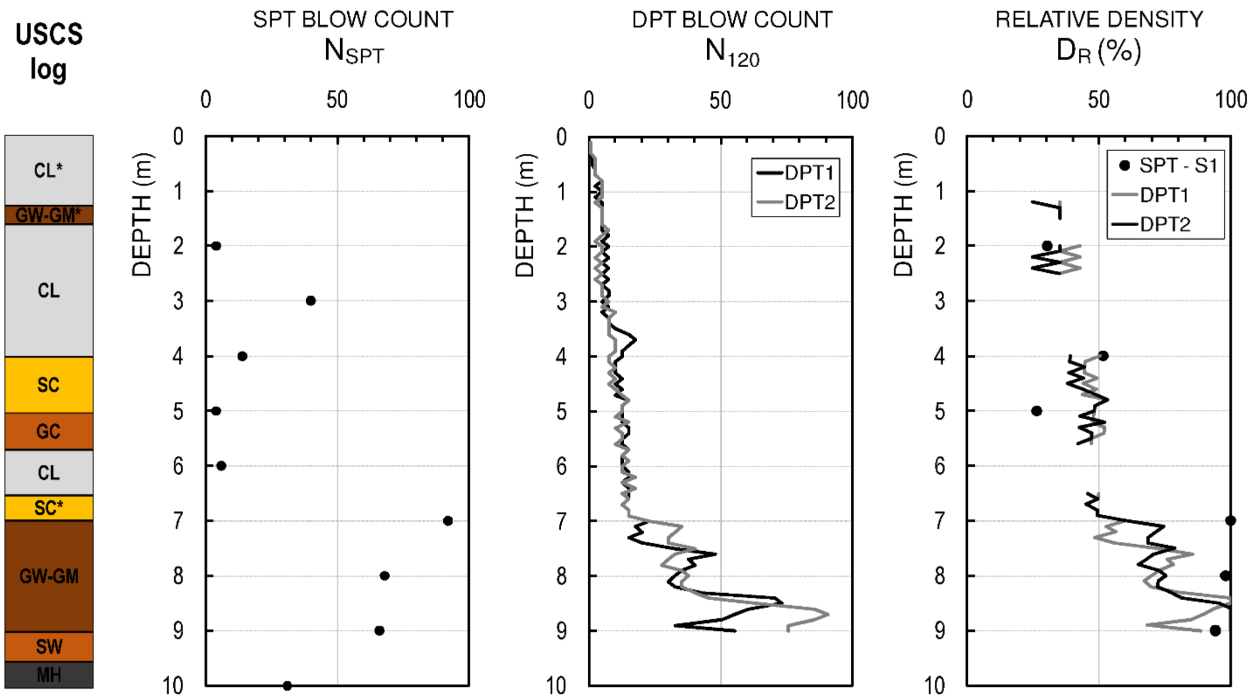

Fig. 8 – Geotechnical stratigraphic log with USCS classification, SPT and DPT blow counts and related relative densities. The star indicates the use of visual-manual procedure for the USCS classification.

Moreover, Fig. 8 includes the relative density (D_R) profiles calculated using the equation proposed by Kulhawy & Mayne (1990) for SPT:

$$D_R = [(N_1)_{60}/60]^{0.5} \tag{7}$$

and by Rollins *et alii* (2021) for DPT:

$$D_R = [N'_{120}/70]^{0.5} \quad (8)$$

Following the geotechnical stratigraphic log in Fig. 8 and the FC values in Table 2, the D_R was calculated only for sandy or gravelly layers. Because of these “border line” values, its thickness, and its position close to the surface, this layer was added to the list of those considered as potentially liquefiable.

The D_R plots in Fig. 8 generally provide consistent results when comparing DPT1 and DPT2; however, they show a clear discrepancy between SPT and DPT estimations in the gravelly layer between 7 and 9 m in depth, probably due to the effect of the particle size that artificially increases the SPT blow counts.

LIQUEFACTION ASSESSMENT AT THE SANTA RUFINA TEST SITE

To evaluate the CSR profile according to the “simplified procedure”, the peak ground acceleration at the ground surface (a_{max}) has been determined starting from the value at outcropping rock conditions (a_g) equal to 0.255g as proposed by Valentini *et alii* (2019) in the Sulmona area for a return period of 475 years based on a fault based PSHA study. Amplification effects due to local soil conditions have been then estimated approximately by considering the stratigraphic amplification factor Ss (as a function of a_g) for the B subsoil class of the Italian building code (NTC, 2018). For $a_{max} = 0.255g$ an Ss value of 1.16 can be estimated leading to a peak ground acceleration at the ground surface $a_{max} = 0.296g$.

To evaluate the $CRR_{7.5}$ based on the SPT, the N_{SPT} values have been corrected following the procedure of Youd *et alii* (2001), considering a measured hammer energy efficiency equal to 65%, a borehole diameter of 101 mm, a rod length of 1.5 m and a standard sampler, to obtain the normalised $(N_1)_{60}$, profile as shown in Fig. 9a. In this respect, it can be noted that the $(N_1)_{60}$ profile presents the minimum values at 2, 4, 5, 6 and 10 m, while it is greater than 50 at 3, 7, 8 and 9 m in depth. To better constrain the results, simplified methods for liquefaction assessment using SPT proposed by Youd *et alii* (2001), Idriss & Boulanger (2008) and Boulanger & Idriss (2014) were used.

As can be seen in Fig. 9a, the $CSR_{7.5,1\,atm}$ data points plotted at approximately one metre depth intervals, using the three different equations gives comparable results for the Youd *et alii* (2001) and Idriss & Boulanger (2008) methods, while the Boulanger & Idriss (2014) method appears substantially different. The $CRR_{7.5}$ values calculated for the SPT values obtained in the layer with a FC of approximately 50% presents an anomalously lower value considering the equation proposed by Idriss & Boulanger (2008). This is also reflected in terms of FS_{liq}, as can be seen in Fig. 9a.

Lastly, the SPT assessment also includes the liquefaction potential index (LPI), calculated as suggested by Iwasaki *et alii* (1978). In this respect, to have an integral measurement in the upper 10 m of depth (assuming that the cohesive soils between 10 and 20 m is not liquefiable), N_{SPT}values were assigned also to those layers potentially liquefiable, but not tested with the SPT because of their limited thickness and position relative to the one-metre test range.

Therefore, considering the stratigraphy and the characteristics of the layers, to the loose gravel from 1.2 to 1.6 m a value of N_{SPT} equal to 4 was associated, according to the SPT tested layer at 2 m in depth, and to the clayey sand from 6.5 to 7 m the N_{SPT} value of 6 was assigned, consistent with the SPT tested layer at 6 m in depth. These attributions were made using the layers identified by the DPT and picking comparable N_{SPT} values based on the correlation with the layers from the DPT and SPT. This artifice makes it possible to partially overcome the limitation of only having SPT values at one metre intervals. This process identified four potentially liquefiable layers (from 1.2 to 1.6 m, from 2 to 2.6 m, from 5 to 5.7 m and from 6.5 to 7 m in depth) to provide reasonable LPI estimations, all in the range of high liquefaction potential, with higher values computed using the method proposed by Boulanger & Idriss (2014), $LPI = 8.9$, compared to that by Youd *et alii* (2001), $LPI = 5.9$.

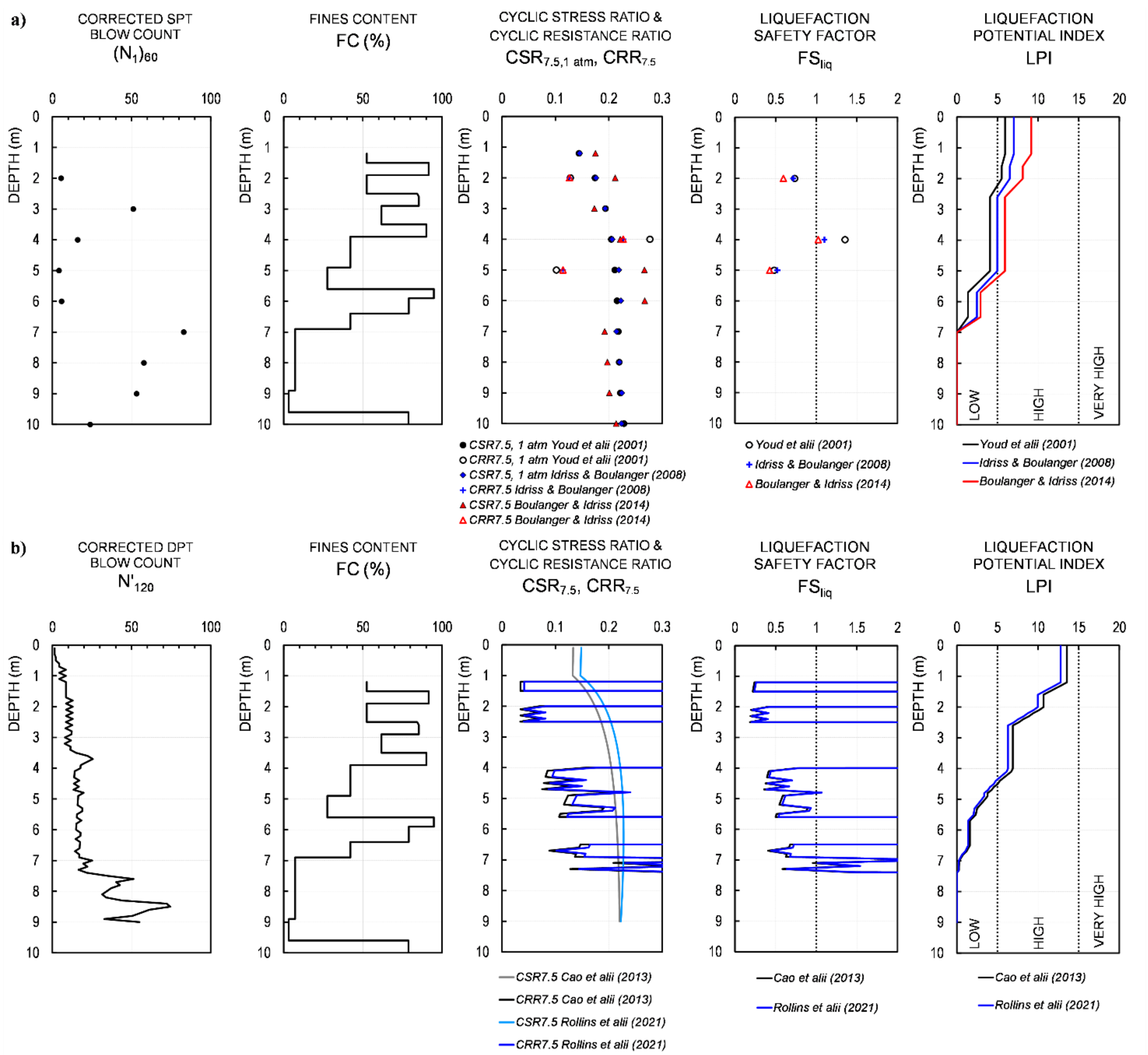

Fig. 9 – (a) Liquefaction assessment results based on SPT methods by Youd *et alii* (2001), Idriss and Boulanger (2008), and Boulanger and Idriss (2014) at Santa Rufina test site; (b) – Liquefaction assessment results based on DPT methods by Cao *et alii* (2013) and Rollins *et alii* (2021) at Santa Rufina test site. Data refers to DPT1.

For the liquefaction assessment using DPT data, both the methods proposed by Cao *et alii* (2013) and that by Rollins *et alii* (2021) are presented, with reference to only DPT1, considering the similarity of the two DPT profiles (see Fig. 8). In making these assessments, the $P_L = 15\%$ curves were used to obtain $CRR_{7.5}$using formulas given by Eqs. 2 and 6, respectively.

Fig. 9b shows that the profiles of the corrected DPT blow counts (N'_{120}) result in the same values for Cao *et alii* (2013) and Rollins *et alii* (2021), despite the minor differences in formulation (see Eqs. 1 and 3). The factors of safety computed by both methods were also very similar for this site. Gravelly and sandy layers with the lowest DPT resistance below the GWT are considered the most critical liquefaction zones. Using $P_L = 15\%$ in the $\mathrm{CRR}_{7.5}$ formulas (see Eqs. 2 and 6) the LPI profiles in Fig. 9b were obtained. The two DPT methods appear to be providing similar $LPI \approx 13$, in the range of high liquefaction potential.

Cubrinovsky *et alii* (2018) observed the effects of the 2016 M_W 7.8 Kaikoura earthquake on 32 sites where simplified methods predicted liquefaction; however, only 15 showed signs of surface effects of liquefaction, while the other 17 did not. In that study, they highlight that the penetration resistance profile did not properly discriminate between the sites where liquefaction did or did not manifest. The 17 sites that did not produce surface effects of liquefaction exhibited a stratigraphy of interbedded liquefiable and non-liquefiable layers, with the presence of separate liquefiable layers located from 7 to 10 m, much below the "critical layer". Liquefaction of these deeper layers likely reduced the potential of pore pressure generation in the critical zone (Cubrinovsky *et alii*, 2018) and reduced permeability in the interbedded zone may have impeded ejecta flow to the surface. On the other hand, the 15 sites that manifested surface liquefaction were characterised by more continuous, thicker, and uniform liquefiable layers. The stratigraphic profile with interbedded liquefiable and non-liquefiable layers may be clearly identified at the Santa Rufina site.

Further observations can be made using laboratory "screening" liquefaction criteria proposed by Idriss & Boulanger (2008) and Andrews & Martin (2000), who respectively plot the PI versus the Liquid Limit (LL) and the LL versus the percentage of particles finer than 2 μm to identify layers susceptible to liquefaction. Figs. 10a and 10b show the plot of the 13 samples from the Santa Rufina test site according to the Idriss & Boulanger (2008) and Andrews & Martin (2000) charts, respectively. For the PI vs LL chart, all samples fall in the clay-like behaviour area, therefore indicating that they are not susceptible to liquefaction. In the LL vs finer than 2 μm chart, most of the samples also fall in the zone indicating no susceptibility to liquefaction, except CD1 and CD9, for which further studies are required, and for samples CD3 and CD4, that are very close to the boundary indicating susceptibility to liquefaction.

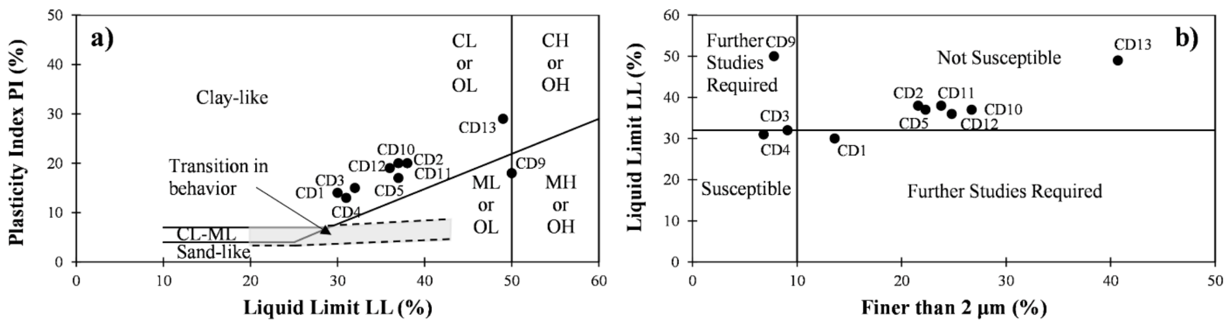

Fig. 10 – Santa Rufina test site: liquefaction screening criteria according to the charts by (a) – Idriss and Boulanger (2008) and (b) – Andrews & Martin (2000).

Based on these considerations, the liquefaction assessment by *in-situ* tests was revised by identifying as non-liquefiable: (1) thin liquefiable layers interbedded within non-liquefiable layers and (2) potentially liquefiable layers classified with a "clay-like" behaviour. As reported in Table 3, this means that the liquefaction potential for this site passes from high (case "A") to low (case "B") for all simplified methods, radically changing the prediction of liquefaction occurrence. The only remaining liquefiable layer is at depth between 7 and 9 m.

Table 3 – Santa Rufina test site: comparison of LPI results obtained using only in situ tests and FC measurements (case "A"), and using in situ tests, FC and PI measurements, excluding interbedded layers (case "B").

In situ test	***Method***	***LPI (case "A")***	***LPI (case "B")***
SPT	Youd *et alii* (2001)	5.9	0.0
	Idriss and Boulanger (2008)	7.0	0.0
	Boulanger and Idriss (2014)	8.9	0.0
DPT	Cao *et alii* (2013)	13.5	0.3
	Rollins *et alii* (2021)	12.8	0.2

CONCLUSIONS

The case history database of gravel liquefaction from around the world clearly indicates the gravelly soils can liquefy and this possibility should be considered in seismic hazard investigations. The data collected and reported in this study also highlight the fact that liquefaction in gravelly soils can be triggered not only by strong/major earthquakes, but also by moderate ($M_W < 6$) seismic events. This point is illustrated by gravel liquefaction after the M_W 5.3 aftershock of the 1976-1977 Friuli (Italy) seismic sequence and by gravel liquefaction in the M_W 5.5 2017 Pohang (South Korea) earthquake.

Liquefied soils typically include well-graded sandy gravel (GW), containing between 14 and 82% gravel with fines content no greater than 22%. In addition, the sand content was typically greater than about 30%. Although the typical gradation curves for liquefiable gravels fall outside the typical range for liquefiable sands sometime used in national codes, this discrepancy should not be used to preclude liquefaction assessments in these soils.

Gravels are often thought to have permeabilities high enough (> 0.004 m/s) that excess pore pressures would dissipate as fast as they generate in an earthquake (Seed *et alii,* 1976). However, for gravels containing more than 30% sand size particles, the permeability would likely be controlled by the D_{10} size of the sand, making the sandy gravel susceptible to liquefaction. Even for gravel sites with higher hydraulic conductivities, the presence of a low-permeability surface layer could impede drainage and make the gravel susceptible to liquefaction (Cao *et alii*, 2013).

The magnitude versus epicentral distance for gravel liquefaction sites is generally in good agreement with boundaries based on the liquefaction of sandy soil. Although this database is limited to 27 historical events and should be expanded, also with paleoseismological data, it is reasonable to consider that the maximum epicentral distance at which gravel liquefaction may occur will be about the same as sand for a given magnitude, M_W.

The site of Santa Rufina, within the Sulmona basin which experienced both sand liquefaction (during the M_W 6.1, 2019 L'Aquila earthquake) and gravel liquefaction (based on paleoseismological evidence, although more detailed analyses are required), provided a good case study, since it is characterised by an alluvial Upper Pleistocene – Holocene profile that consists both of sandy-silty and gravelly-sand alternating layers, with high vertical and lateral variability. This variability in stratigraphy, typical of many sedimentary basins, introduce relevant uncertainties in the regional extensions of the liquefaction risk assessment at discrete vertical profiles with simplified methods. This highlights the need for more detailed geotechnical and geological studies in liquefaction assessment at regional scale (e.g., microzonation studies).

Furthermore, the case study highlighted that the SPT-based liquefaction triggering procedure applied to a site with vertically alternating thin layers composed of fine and coarse particles has three major limitations with the respect to the DPT-based analyses: (1) as SPT sounding is not generally continuous, it may not provide important information about thin layers; (2) due to the penetrometer diameter, the SPT may overestimate the D_R in layers containing coarse particles; and (3) the DPT approach is directly based on field performance of gravels whereas other methods assess gravel liquefaction based on methods developed for sand. Considering these shortcomings, the SPT-based procedure may underestimate the liquefaction potential at such sites. In conclusion, SPT and DPT based methods may provide conflicting results in alternating soil stratigraphy, such as the Santa Rufina site. The exclusion of liquefiable layers between interbedded cohesive layers (e.g., layers characterised by a "clay-like" behaviour according to well-known screening criteria) can refine the *in-situ* assessment, shifting the LPI values to approximately zero. In this respect, the availability of a borehole log and standard geotechnical laboratory information provides fundamental and complementary data critical to achieving a reliable assessment of the liquefaction hazard at such complex sites.

Our results suggest how liquefaction hazard analyses in active seismic regions should be carried out considering gravel as potentially liquefiable. However, further studies are required to better constrain these results and to investigate the role of the geological context in liquefaction phenomena.

SUPPLEMENTAL MATERIAL

The online version contains supplemental material (Table S1).

ACKNOWLEDGEMENTS

This study was carried out in the framework of the ReLUIS-DPC 2019–2021 research project under funding of the Italian Civil Protection Department (Task 16.1 Site Response and Liquefaction). Additional funding by Regione Abruzzo is also acknowledged. The Authors thank Nicola Sciarra and Gabriele Toro for their support in the geotechnical analyses at the Laboratory of University of Chieti-Pescara and Marco Francescone and Ylenia Zaccagnini for their precious help during the situ surveys. Domenico Trotta is also thanked for providing data of SB borehole.

Partial funding provided by grant CMMI-1663546 from the U.S. National Science Foundation. This funding is gratefully acknowledged. However, the opinions, conclusions and recommendations in this paper do not necessarily represent those of the sponsors.

REFERENCES

Ambraseys N.N. (1988) – *Engineering seismology.* Earthquake Engineering & Structural Dynamics, **17** (1), 1-105. https://doi.org/10.1002/eqe.4290170101

Amoroso S., Milana G., Rollins K.M., Comina C., Minarelli L., Manuel M.R., Monaco P., Franceschini M., Anzidei M., Lusvardi C., Cantore L., Carpena A., Casadei S., Cinti F.R., Civico R., Cox B.R., De Martini P.M., Di Giulio G., Di Naccio D., Di Stefano G., Facciorusso J., Famiani D., Fiorelli F., Fontana D., Foti S., Madiai C., Marangoni V., Marchetti D., Marchetti S.L., Martelli L., Mariotti M., Muscolino E., Pancaldi D., Pantosti D., Passeri F., Pesci A., Romeo G., Sapia V., Smedile A., Stefani M., Tarabusi G., Teza G., Vassallo M., Villani F. (2017) – *The first Italian blast-induced liquefaction test (Mirabello, Emilia-Romagna, Italy): description of the experiment and preliminary results.* Ann. Geophys., **60** (5), S0556. https://doi.org/10.4401/ag-7415

Amoroso S., Rollins K.M., Andersen P., Gottardi G., Tonni L., García Martínez M.F., Wissmann K.J., Minarelli L., Comina C., Fontana D., De Martini P.M., Monaco P., Pesci A., Sapia V., Vassallo M., Anzidei M., Carpena A., Cinti F., Civico R., Coco I., Conforti D., Doumaz F., Giannattasio F., Di Giulio G., Foti S., Loddo F., Lugli S., Manuel M.R., Marchetti D., Mariotti M., Materni V., Metcalfe B., Milana G., Pantosti D., Pesce A., Salocchi A.C., Smedile A., Stefani M., Tarabusi G., Teza G. (2020) – *Blast-induced liquefaction in silty sands for full-scale testing of ground improvement methods: insights from a multidisciplinary study*. Eng Geol, 265: 105437. https://doi.org/10.1016/j.enggeo.2019.105437

Andrews D.C.A., Martin G.R. (2000) – *Criteria for liquefaction of silty soils.* Proceedings, 12th World Conference in Earthquake Engineering, Auckland, New Zealand.

Andrus R.D., Stokoe K.H. (2000) – *Liquefaction resistance of soils from shear-wave velocity.* J. Geotech. Geoenviron. Eng., **126** (11), 1015-1025. https://doi.org/10.1061/(ASCE)1090-0241(2000)126:11(1015)

A.S.T.M. D2488-09 (2009) – *Standard practice for classification of soils for engineering purposes (Visual-Manual Procedure).* ASTM International, West Conshohocken, PA, 12 p.p.

A.S.T.M. D2487-11 (2011) – *Standard practice for description and identification of soils (Unified Soil Classification System).* ASTM International, West Conshohocken, PA, 12 p.p.

Baratta M. (1910) – *La catastrofe sismica Calabro-Messinese (28 dicembre 1908).* Società Geografica Italiana, Roma. [In Italian]

Boulanger R.W., Idriss I.M. (2014) – *CPT and SPT based liquefaction triggering procedure.* Report No. UCD/CGM-14/01, Center for Geotechnical Modelling, Department of Civil and Enviromentally Engineering, Univ. California, California, 134 p.p. https://doi.org/10.1061/(ASCE)GT.1973-5606.0001388

Cao Z., Youd T.L., Yuan X. (2011) - *Gravelly soils that liquefied during 2008 Wenchuan, China earthquake,* $M_s=8$. Soil Dyn. Earthq. Eng., **31**, 1132-1143. https://doi.org/10.1016/j.soildyn.2011.04.001

Cao Z., Youd T.L., Yuan X. (2013) – *Chinese dynamic penetration test for liquefaction evaluation in gravelly soils.* J. Geotech. Geoenviron. Eng., **139** (8), 1320-1333. https://doi.org/10.1061/(ASCE)GT.1943-5606.0000857

Castilla R.A., Audemard F.A. (2007) – *Sand blows as a potential tool for magnitude estimation of pre-instrumental earthquakes.* J. Seismol., **11**, 473-487. https://doi.org/10.1007/s10950-007-9065-z

Ceccaroni E., Ameri G., Capera A.A.G., Galadini F. (2009) – *The 2nd century AD earthquake in central Italy: archeoseismological data and seismotectonic implications.* Nat. Hazards, **50**, 335-359. https://doi.org/10.1007/s11069-009-9343-x

Chinese Design Code (2021) – *Design code for buildings foundation of Chengdu region.* DB51/T5026-2001, Administration of Quality and Technology, Chengdu, China. [In Chinese]

Cubrinovsky M., Bray J.D., de la Torre C., Olsen M., Bradley B., Chiaro G., Stocks E., Wotherspoon L., Krall T. (2018) – *Liquefaction-induced damage and CPT characterization of the reclamations at CentrePort, Wellington.* Bull. Seismol. Soc. Am., **108** (3B), 1695-1708. https://doi.org/10.1785/0120170246

Daniel C.R., Howie J.A., Sy A. (2003) – *A method for correlating large penetration test (LPT) to standard penetration test (SPT) blow counts.* Can. Geotech. J., **40**, 66-77. https://doi.org/10.1139/t02-094Galli P. (2000) – *New empirical relationship between magnitude and distance for liquefaction*. Tectonophysics, **324**, 169-187. https://doi.org/10.1016/S0040-1951(00)00118-9

Galli P., Giaccio B., Peronace E., Messina P. (2015) – *Holocene paleoearthquakes and Early-Late Pleistocene slip rate on the Sulmona Fault (Central Apennines, Italy)*. Bull. Seismol. Soc. Am., **105** (1), 1-13. https://doi.org/10.1785/0120140029

Giaccio B., Castorina F., Nomade S., Scardia G., Voltaggio M., Sagnotti L. (2013) – *Revised chronology of the Sulmona lacustrine succession, central Italy*. J. Quat. Sci., **28** (6), 545-551. https://doi.org/10.1002/jqs.2647

Gori, S., Giaccio, B., Galadini, F., Falcucci, E., Messina, P., Sposato, A., Dramis, F. (2011) - *Active normal faulting along the Mt. Morrone south-western slopes (central Apennines, Italy).* International journal of earth sciences, 100(1), 157-171. https://doi.org/10.1007/s00531-009-0505-6

Idriss I.M., Boulanger R.W. (2008) – *Soil liquefaction during earthquakes*. Earthquake Engineering Research Institute, Oakland, CA, 237 p.p.

IWASAKI T., TATSUOKA F., TOKIDA K., YASUDA S. (1978) – *A practical method for assessing soil liquefaction potential based on case studies at various sites in Japan*. 2nd International Conference on Microzonation for Safer Construction Research and Application, 885-896. https://doi.org/10.1016/0261-7277(84)90027-5

KAYEN R., MOSS R.E.S., THOMPSON E.M., SEED R.B., CETIN K.O., KIUREGHIAN A.D., TANAKA Y., TOKIMATSU K. (2013) – *Shear-wave velocity-based probabilistic and deterministic assessment of seismic soil liquefaction potential*. J. Geotech. Geoenviron. Eng., **139** (3), 407-419. https://doi.org/10.1061/(ASCE)GT.1943-5606.0000743

KOKUSHO T., YOSHIDA Y. (1997) – *SPT N-value and S-wave velocity for gravelly soils with different grain size distribution.* Soils Found. **37** (4), 105-113. https://doi.org/10.3208/sandf.37.4_105

KULHAWY F.H., MAYNE P.W. (1990) – *Manual on estimating soil properties for foundation design*. EPRI Report EL-6800, 306 p.p.

LIAO S.S.C., VENAZIANO D., WHITMAN R.V. (1988) - *Regression models for evaluating liquefaction probability.* J. Geotech. Eng., **114** (4), 389-411. https://doi.org/10.1061/(ASCE)0733-9410(1988)114:4(389)

MAURER B.W., GREEN R.A., QUIGLEY M.C., BASTIN S. (2015) – *Developed of magnitude-bound relations for paleoliquefaction analyses: New Zealand case study.* Eng. Geology, **197**, 253-266. https://doi.org/10.1016/j.enggeo.2015.08.023

MAYNE P.W., COOP M.R., SPRINGMAN S.M., HUANG A., ZORNBERG J.G. (2009) – *Geomaterial behavior and testing.* Proceedings of the 17th International Conference on Soil Mechanics and Geotechnical Engineering, 2777-2873.

MICCADEI E., BARBERI R., CAVINATO G.P. (1998) – *La geologia quaternaria della conca di Sulmona (Abruzzo, Italia centrale).* Geologica Romana, **34**, 59-86. [In Italian]

MONACO P., SANTUCCI DE MAGISTRIS F., GRASSO S., MARCHETTI S., MAUGERI M., TOTANI G. (2011) – *Analysis of the liquefaction phenomena in the village of Vittorito (L'Aquila).* Bull. Earthq. Eng., **9**, 231-261. https://doi.org/10.1007/s10518-010-9228-0

NAIK S.P., KIM Y.S., KIM T., SU-HO J. (2019) – *Geological and structural control on localized basin during the Pohang earthquake (M_W 5.4, 15th November 2017), South Korea.* Geosciences, **9** (4), https://doi.org/10.3390/geosciences9040173

NTC (2018) – *Aggiornamento delle "Norme tecniche per le costruzioni".* D.M. 17 gennaio 2018, pubblicato sul Supplemento ordinario alla Gazzetta Ufficiale, n.42 del 20 febbraio 2018, Serie generale. [In Italian]

OBERMEIER S.F. (1996) - *Use of liquefaction-induced features for paleoseismic analysis – An overview of how seismic liquefaction features can be distinguished from other features and how their regional distribution and properties of source sediment can be used to infer the location and strength of Holocene paleo-earthquakes.* Engineering Geology, **44**, 1-76. https://doi.org/10.1016/S0013-7952(96)00040-3

Pizzi, A., Miccadei, E., Piacentini, T., Pipponzi, G., Galadini, F., Luzi, L. (2014) - *Microzonazione simica di Livello 1 del Comune di Sulmona (AQ), Relazione illustrativa con carte e sezioni allegate*. Regione Abruzzo – Dip. Protezione Civile, https://protezionecivile.regione.abruzzo.it/index.php/microzonazione.

Pizzi A., Calamita F., Coltorti M., Pieruccini P. (2002) – *Quaternary normal faults, intramontane basins and seismicity in the Umbria-Marche-Abruzzi Apennine Ridge (Italy): contribution of neotectonic analysis to seismic hazard assessment.* Boll. Soc. Geol. It., Special Issue 1, 923-929.

Rodriguez-Pascua M.A., Calvo J.P., De Vicente G., Gómez-Gras D. (2020) – *Soft sediment deformation structures interpreted as seismites in lacustrine sediments of the Prebetic Zone, SE Spain, and their potential use as indicators of earthquake magnitudes during the Late Miocene.* Sediment. Geol., **135**, 117-135. https://doi.org/10.1016/S0037-0738(00)00067-1

Rollins K.M., Amoroso S., Milana G., Minarelli L., Vassallo M., Di Giulio G. (2020) – *Gravel liquefaction assessment using the dynamic cone penetration test based on field performance from the 1976 Friuli Earthquake.* J. Geotech. Geoenviron. Eng., **146** (6). https://doi.org/10.1061/(asce)gt.1943-5606.0002252

Rollins K.M., Roy J., Athanasopoulos-Zekkos A., Zekkos D., Amoroso S., Cao Z. (2021) – *A new dynamic cone penetration test-based procedure for liquefaction triggering assessment of gravelly soils.* J. Geotech. Geoenviron. Eng., **147** (12). https://doi.org/10.1061/(ASCE)GT.1943-5606.0002686

Rollins K.M., Roy J., Athanasopoulos-Zekkos A., Zekkos D., Amoroso S., Cao Z., Milana G., Vassallo M., Di Giulio G. (2022) – *A new V_S-based liquefaction triggering procedure for gravelly soils.* J. Geotech. Geoenviron. Eng., **148** (6). https://doi.org/10.1061/(ASCE)GT.1943-5606.0002784

Rovida A., Locati M., Camassi R., Lolli B., Gasperini P., Antonucci A. (2022) – *Catalogo parametrico dei terremoti italiani (CPTI15), versione 4.0.* Istituto Nazionale di Geofisica e Vulcanologia (INGV). https://doi.org/10.13127/CPTI/CPTI15.4

Salocchi A.C., Minarelli L., Lugli S., Amoroso S., Rollins K.M., Fontana D. (2020) – *Liquefaction source layer for sand blows induced by the 2016 megathrust earthquake (M_W 7.8) in Ecuador (Boca de Briceño)*. J. South Am. Earth Sci., **103**. https://doi.org/10.1016/j.jsames.2020.102737

Seed H.B., Idriss I.M. (1971) – *Simplified procedure for evaluating soil liquefaction potential*. J. Soil Mech. Found. Div., **97** (9), 1249-1273. https://doi.org/10.1061/JSFEAQ.0001662

Seed, H. B., Martin, P. P. and Lysmer, J. (1976) – *The generation and dissipation of pore water pressure changes during soil liquefaction*. Journal of the Geotechnical Engineering Division, **102** (4), 323-346.

Sirovich L. (1996a) – *In-situ testing of repeatedly liquefied gravels and liquefied overconsolidated sands*. Soil Found., **36** (4), 35-44.

TOKIMATSU K., YOSHIMI Y. (1983) - *Empirical correlation of soil liquefaction based on SPT N-value and fines content*. Soils Found., **23** (4), 56-74. https://doi.org/10.3208/sandf1972.23.4_56

TSUCHIDA H., HAYASHI S. (1971) - *Estimation of liquefaction potential of sandy soils*. Proceedings of the 3rd Joint Meeting, US–Japan Panel on Wind and Seismic Effects, May 1971. UJNR, Tokyo, 91-109.

VALENTINI A., PACE B., BONCIO P., VISINI F., PAGLIAROLI A., PERGALANI F. (2019) – *Definition of seismic input from fault-based PSHA: remarks after the 2016 central Italy earthquake sequence*. Tectonics, **38**, 595-620. https://doi.org/10.1029/2018TC005086

YOUD T.L., IDRISS I.M., ANDRUS R.D., ARANGO I., CASTRO G., CHRISTIAN J.T., DOBRY R., FINN W.D.L., HARDER L.F., HYNES M.E., ISHIHARA K., KOESTER J.P., LIAO S.S.C., MARCUSON W.F., MARTIN G.R., MITCHELL J.K., MORIWARI YOSHIHARU, POWER M.S., ROBERTSON P.K., SEED R.B., STOKOE K.H. (2001) – *Liquefaction resistance of soils: summary report from the 1996 NCEER and 1998 NCEER/NSF workshops on evaluation of liquefaction resistance of soils*. J. Geotech. and Geoenviron. Eng., **127** (10), 817-833. https://doi.org/10.1061/(ASCE)1090-0241(2001)127:10(817)